PUBLISHED VERSION

Zack Y. Shan, Richard Kwiatek, Richard Burnet, Peter Del Fante, Donald R. Staines, Sonya M. Marshall-Gradisnik and Leighton R. Barnden

Progressive brain changes in patients with chronic fatigue syndrome: a longitudinal MRI study

Journal of Magnetic Resonance Imaging, 2016; 44(5):1301-1311

Originally published at:
http://doi.org/10.1002/jmri.25283

Progressive Brain Changes in Patients With Chronic Fatigue Syndrome: A Longitudinal MRI Study

Zack Y. Shan, PhD,[1]* Richard Kwiatek, MBBS,[2] Richard Burnet, MBBS,[3]
Peter Del Fante, MBBS,[4] Donald R. Staines, MBBS,[1]
Sonya M. Marshall-Gradisnik, PhD,[1] and Leighton R. Barnden, PhD[1]

Purpose: To examine progressive brain changes associated with chronic fatigue syndrome (CFS).
Materials and Methods: We investigated progressive brain changes with longitudinal MRI in 15 CFS and 10 normal controls (NCs) scanned twice 6 years apart on the same 1.5 Tesla (T) scanner. MR images yielded gray matter (GM) volumes, white matter (WM) volumes, and T1- and T2-weighted signal intensities (T1w and T2w). Each participant was characterized with Bell disability scores, and somatic and neurological symptom scores. We tested for differences in *longitudinal* changes between CFS and NC groups, inter group differences between *pooled* CFS and *pooled* NC populations, and correlations between MRI and symptom scores using voxel based morphometry. The analysis methodologies were first optimized using simulated atrophy.
Results: We found a significant decrease in WM volumes in the left inferior fronto-occipital fasciculus (IFOF) in CFS while in NCs it was unchanged (family wise error adjusted cluster level *P* value, $P_{FWE} < 0.05$). This longitudinal finding was consolidated by the group comparisons which detected significantly decreased regional WM volumes in adjacent regions ($P_{FWE} < 0.05$) and decreased GM and blood volumes in contralateral regions ($P_{FWE} < 0.05$). Moreover, the regional GM and WM volumes and T2w in those areas showed significant correlations with CFS symptom scores ($P_{FWE} < 0.05$).
Conclusion: The results suggested that CFS is associated with IFOF WM deficits which continue to deteriorate at an abnormal rate.

J. MAGN. RESON. IMAGING 2016;44:1301–1311.

Chronic fatigue syndrome (CFS), sometimes referred to as myalgic encephalomyelitis (ME), is a debilitating illness with a variety of presenting features. Although prolonged and disabling fatigue is present in 10–25% of patients presenting to general practitioners,[1] a diagnosis of CFS requires that patients experience persistent or relapsing fatigue for at least 6 consecutive months and have four or more of the following symptoms: postexertional malaise, impaired memory or concentration, unrefreshing sleep, muscle pain, multi-joint pain without redness or swelling, tender cervical or axillary lymph nodes, sore throat, and headache.[2,3] Although the cause of CFS remains unknown, altered central nervous system (CNS) function is believed to play an important role,[4] including altered perception of fatigue and pain, deficits in the cognitive functions of concentration and memory, mood changes of depression and anxiety, and sleep disturbance.[1] Accordingly, neuroimaging studies have investigated possible brain changes associated with CFS.[5–8] However, most of the previous neuroimaging studies were cross sectional comparisons of differences between CFS patients and normal controls (NCs) except one longitudinal study that examined white matter (WM) hyperintensities, cerebral blood and cerebrospinal fluid (CSF) flows in scans 1 year apart.[9]

View this article online at wileyonlinelibrary.com. DOI: 10.1002/jmri.25283

Received Feb 18, 2016, and in revised form Apr 1, 2016. Accepted for publication Apr 1, 2016.

*Address reprint requests to: Z.S., National Centre for Neuroimmunology and Emerging Diseases, Menzies Health Institute Queensland, Griffith University, Southport, QLD 4222, Australia. E-mail: z.shan@griffith.edu.au

From the [1]National Centre for Neuroimmunology and Emerging Diseases, Menzies Health Institute Queensland, Griffith University, Southport, Australia; [2]Division of Medical Subspecialities, Lyell McEwin Hospital, Elizabeth Vale, SA, Australia; [3]Endocrinology department, Royal Adelaide Hospital, Adelaide, Australia; and [4]Healthfirst Network, Woodville, Australia

Additional supporting information may be found in the online version of this article.

Longitudinal brain change associated with CFS is of importance in both understanding the pathomechanism and development of CFS and in the evaluation of interventions. One intervention study reported increased gray matter (GM) volume in the lateral frontal lobe in CFS patients who underwent cognitive behavioral therapy (CBT) 10 months after baseline.[10] The authors interpreted this change to be a result of CBT. However, this interpretation is problematic without a knowledge of longitudinal brain changes in the CFS patients without intervention, because the reported changes could also be due to brain plasticity associated with CFS or progression of CFS, instead of the intervention. Continuing brain changes associated with CFS have yet to be investigated. The purpose of this longitudinal study is to evaluate progressive brain changes associated with CFS.

Previous cross-sectional neuroimaging studies of CFS have yielded inconsistent results. One group found significant reductions in *global* GM volumes[6] while others did not.[8,11] One study found a decrease in *regional* GM volume in prefrontal areas,[7] and another found such decreases in the occipital lobe, right angular gyrus, and left parahippocampal gyrus.[12] Cortical thickness was found to be increased in right arcuate fasciculus end points, the middle temporal gyrus, precentral gyri, and occipital lobe,[8] while other studies did not find significant regional GM differences.[6,11] Similarly, inconsistent WM changes have been reported.[8,11–13] Such inconsistency could be due to sample size, proportion of genders, diagnosis criteria, duration of the disease or even the heterogeneous nature of CFS. However, it could be also due to the empirical parameters used in quantitative image processing.

In response to the aforementioned challenges, we designed a longitudinal MRI study to investigate long term brain changes associated with CFS over 6 years using optimized voxel based morphometry (VBM) analysis. The purpose of this study is to (1) optimize VBM methodology for analysis of longitudinal images using simulated atrophy, (2) investigate longitudinal brain changes in patients with CFS, (3) detect brain structural differences between CFS and NCs, and (4) identify correlations in CFS between structural differences and disease severity measures.

Materials and Methods

Subjects

The subjects were recruited based on availability, from 25 subjects with CFS and 25 NCs from a previous cross-sectional study.[14] The initial recruitment of the CFS group was from community-based specialist and general practice. They met both the Fukuda[3] and Canadian[2] criteria. Their assessment was detailed in a previous report.[11] After approximately 6 years, 15 of the subjects with CFS, aged 34.06 ± 8.77 (mean ± SD) at first evaluation, and 10 NC subjects, aged 30.5 ± 7.93 at first evaluation, could be contacted and agreed to participate in a repeat longitudinal evaluation. The time intervals between the two evaluations for CFS and NCs were 6.43 ± 0.57 and 6.21 ± 0.31 years, respectively. No CFS or NC subject had developed a significant medical, including hypertension, or psychiatric illness in the intervening years. One CFS and one NC subject had remained on thyroxine to treat hypothyroidism, which predated their involvement in the initial study. Three CFS subjects were taking antidepressants and were requested to stop these for 1 week before their MRI scans. No subject was otherwise taking centrally acting medication. In both CFS and NC subjects, there was no significance change in weight across time. There were four CFS males (male to female ratio = 0.36) and two NC males (male to female ratio = 0.25). There was no significant difference in age ($P = 0.20$) or time interval ($P = 0.27$) between the CFS and NC groups. All subjects were right-handed, not smokers, nor substance abusers.

CFS severity was measured by three scores: the Bell CFS disability score,[15] a somatic symptom score (Somatic SS), and a neurological symptom score (Neuro SS).[14] The Somatic and Neuro SS were derived from self-scores of the 10 most significant symptoms.[16] The Somatic SS was the sum of the six self-scores for severity of fatigue, change in sleeping patterns, dizziness on standing, pain in muscles, stomach symptoms, and overall level of function. The Neuro SS was the sum of four self-scores for change in concentration, change in short-term memory, headaches, and experience of emotional swings. All three symptom scores are inversely proportional to the severity of the disease, i.e., lower scores indicate more severe disease. To determine their levels of depression and anxiety, all subjects completed the Hospital Anxiety and Depression Scale (HADS) questionnaire.[17] The HADS questionnaire was used in this study because it has been proved to be a reliable and simple test and patients have no difficulty in understanding the reason to answer the questionnaire.

The study protocol was approved by the Human Research Ethics Committee of The Queen Elizabeth Hospital in compliance with the Australia National Statement on Ethical Conduct in Human Research, and all subjects gave informed written consent for both examinations.

MRI Acquisition

MR images at both time points were acquired on a Philips 1.5 Tesla (T) Intera MR scanner (Philips, Eindhoven, the Netherlands) with a body transmit coil and birdcage receive coil. Transverse anatomic images were acquired using a three-dimensional spoiled gradient-echo sequence with TR = 5.76 ms, TE = 1.9 ms, flip angle = 9°, resolution = 0.938 × 0.938 × 1 mm^3. Transverse T1 weighted spin echo MR images with contiguous slices of 0.82 × 0.82 × 3 mm^3 were acquired with TR = 600 ms, TE = 15 ms, flip angle = 90°. Transverse T2 weighted spin echo MR images with contiguous slices of 0.82 × 0.82 × 3 mm^3 were acquired with TR = 4000 ms, TE = 80 ms, flip angle = 90°.

Segmentation and Validation

The three-dimensional anatomic images were segmented into GM, WM, CSF, and extra-cerebral tissue using SPM12 (Wellcome Trust Centre for Neuroimaging, London, UK), in which a unified probabilistic framework that combined image segmentation, tissue classification, and bias correction within the same generative model was

implemented.[18] In SPM12, the unified segmentation incorporates a few iterations of a simple Markov Random Field (MRF) cleanup procedure to remove isolated voxel assignments. Optimization of the user-specified parameter that controls the strength of the MRF is described in the Supplementary Material, which is available online. As a result anatomical images from CFS and NC were segmented with the MRF value of 4. Global GM and WM volumes were computed in SPM12 by summing all voxel values in the GM and WM images accounting for the voxel volumes.

Statistical Analysis of Longitudinal Changes in Clinical Measures and Global Volumes

Longitudinal changes in each group and inter-group differences in the clinical measures (Bell CFS disability score, Somatic SS, Neuro SS, anxiety and depression from HADS) and global GM and WM volumes were tested using SPSS22 (IBM, New York).

Paired two tailed t-tests were used to test for equality of means and to compare longitudinal changes in the clinical measures, global GM volumes, and global WM volumes in both the CFS and NC groups. Correlation coefficients between time point 1 and time point 2 values for the clinical measures, global GM volumes, and global WM volumes, were tested for a significant difference from zero. Bonferroni correction for multiple comparisons of the seven characteristics (five symptom measures and two brain volumes) was used to determine uncorrected ($P < 0.05$) and corrected ($P < 0.0071$) statistical significance.

The clinical measures and global GM and WM volumes of the CFS and NC groups *pooled* over the two times were compared using an independent two group t-test. Two-tailed tests for equality of means with unequal group variances were followed by Bonferroni correction for multiple comparisons of eight characteristics (five symptom measures, one age, and two brain volumes) to determine uncorrected ($P < 0.05$) and corrected ($P < 0.0062$). Pearson correlations between each clinical measure and global GM and WM volumes from all subjects were calculated. Bivariate tests of significant difference in correlation coefficient from zero with two tails were followed with Bonferroni correction for multiple comparisons of 21 pairs to test for uncorrected ($P < 0.05$) and corrected ($P < 0.0023$) statistical significance.

Assessment of VBM Options Using Simulated Atrophy

VBM derives images of relative GM and WM volumes from structural MR images, which can then be subjected to voxel-wise statistical analysis in cross-sectional or longitudinal studies. VBM is a well-established tool to examine patterns of regional brain changes in neurological diseases and neuroanatomical correlates of CNS diseases. Although much VBM preprocessing and analysis is automated in SPM, many methodological options remain for user selection,[19] including selection or creation of templates, registration algorithms, and comparison strategies.

To optimize and test the VBM methodology options, we used an atrophy simulation tool with a topology preserving transformation model.[20] MR images from 25 normal controls were used for the simulation study. Tool inputs were the original image, its segmentation, location of the atrophy center, and the radius of the atrophy sphere. The tool simulates atrophy by finding a dense warping deformation that produces the specified levels of volumetric loss on the labelled tissue using an energy minimization strategy. The topology of tissue morphology is preserved in the simulation (Fig. 1). We selected the atrophy center on the axial slice at the level of the inferior colliculus and, within that slice, in WM at the anterior pole of the left cerebral peduncle. The center was defined manually for each subject in native space. (Fig. 1 shows this location in two subjects each with two atrophy levels). This region was chosen to mimic the atrophy reported in one of our previous studies.[11] Atrophy spheres (radius = 5 mm) with three levels of atrophy (5%, 3%, and 1%) were applied.

The original images and images with simulated atrophy represent images at time points 1 and 2 in a longitudinal study. Six methodological options were considered. Smoothing was performed with an 8 mm × 8 mm × 8 mm full-width half-maximum Gaussian filter for all options. All used processing modules implemented in SPM12.

1. DARTEL DN directly normalizes individual images into MNI (Montreal Neurological Institute) space (Supp. Fig. S1). (a) All 3D anatomic images were segmented into GM and WM partitions using a unified segmentation framework[18] with the optimized MRF parameter. (b) For each individual, the deformation of their GM image to MNI space was computed using DARTEL (diffeomorphic anatomical registration through exponentiated lie algebra) nonlinear registration and recorded as flow field image.[21] This procedure was implemented in SPM12 by means of "Run Dartel (existing template)". (c) The flow field images were then used to normalize GM and WM images to MNI space and generate smoothed, spatially normalized, and modulated images. The latter encode the local volume changes associated with the nonlinear deformation, by means of Jacobian scaling, into image intensities. (d) Finally, the preprocessed WM images at time point 1 were compared with those from time point 2 using an SPM12 (parametric) paired t-test.
2. DARTEL ST (study specific template) is the same as option 1 except that a study-specific GM template was created in (b) (Supp. Fig. S1). This involves iteratively matching all images to a template generated from their own means, It was implemented by means of "Run Dartel (create template)" in SPM12. The study-specific template is then normalized to MNI space in step 1(c). Two deformations, the flow field images representing individual image to study-specific template and the transformations of the template to MNI space, were combined and encoded in modulated images.
3. SHOOT ST is the same as option 2 except that the two implementations of DARTEL were replaced by a diffeomorphic registration using geodesic shooting and Gauss-Newton optimization[22] (Supp. Fig. S1).
4. DARTEL SnPM is the same as option 2 except that a nonparametric paired t-test[23] was used in step (d) (Supp. Fig. S1).
5. LD (longitudinal difference) first creates within-subject templates (Supp. Fig. S2). (a) Raw images from the 1st and 2nd time points were aligned to MNI space using a rigid body registration. (b) For each subject, these aligned images were averaged to create the subject template. (c) Raw images from

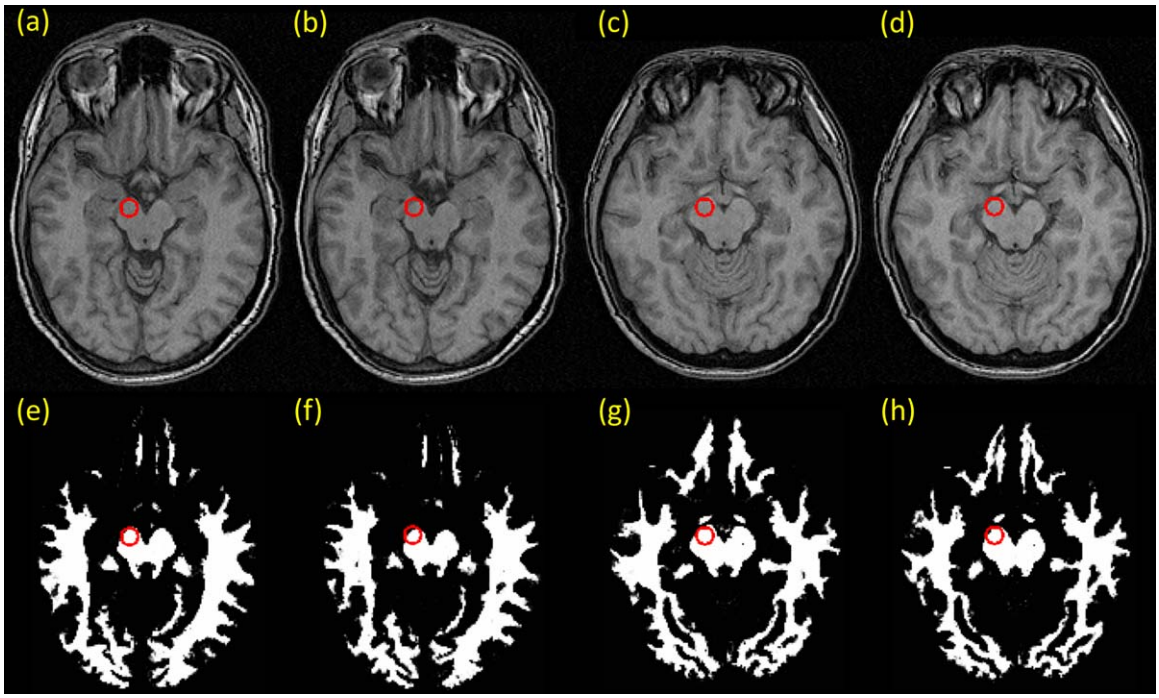

FIGURE 1: Illustration of atrophy simulation in two subjects. A representative axial slice at the center of the atrophy sphere is shown with and without simulated atrophy. Red circles are used to show the location of the atrophy only. The circle radius has no relationship to the radius of the atrophy sphere or atrophy rate. All images are in their native space. a,e,c,g: Respectively, the original raw and WM images without change from two subjects. b,f,d,h: Respectively, the raw and WM images with 5% simulated atrophy in the left midbrain. Atrophy can be seen at the edge of segmented WM images while topologies of deformed structures were preserved (f,h).

1st and 2nd time points were then aligned to this subject template. (d) Aligned images from step (c) were preprocessed using the same procedures as option 2. (e) Difference images were calculated by subtracting the preprocessed image of time point 2 from that of time point 1. (f) Difference images from step (e) were compared using a one sample parametric t-test.

6. LJD (longitudinal Jacobian difference) creates a within-subject template differently to option 5 (Supp. Fig. S2). (a) A symmetric diffeomorphic modelling of longitudinal data[24] was used to create a mid-point image by estimating the optimal mapping between the template and each of the images by means of "Pairwise Longitudinal Registration" in SPM12. A Jacobian difference image records the difference of the Jacobian map for deformation from the mid-point image to the first scan and this to the second scan. (b) The mid-point (mean) image was segmented into GM, WM and CSF images. (c) GM images from step (b) were used to create a study-specific template using DARTEL. (d) The Jacobian difference images from step (a) were multiplied by the GM image from step (b). (e) The difference images from step (d) were normalized to MNI space and smoothed. (f) Difference images from step (e) were compared using a one sample SPM12 (parametric) t-test.

The simulated atrophy images were analyzed using SPM12 with the above six VBM methodology options. To evaluate the sensitivity of each option, different randomly selected sample sizes (N = 25, 20, 15, 10) for each level of atrophy were compared with the original images from the same subjects with the six VBM options. Statistical significance was determined using family wise error (FWE) corrected voxel level $P < 0.05$. Significant clusters with more than 25 voxels and less than 25 voxels that overlapped the simulated atrophy were defined as true positive (TP) and small true positive (STP), respectively. Significant clusters that were found at different locations from the simulated atrophy were defined as false positive (FP). Failure to detect simulated atrophy was defined as false negative (FN) (Supp. Fig. S3).

VBM Preprocessing of Longitudinal MR Data From CFS Patients and NCs

Anatomic MR images from CFS and NC were preprocessed using the optimum VBM LD methodological option (5a-5e). Images of T1 and T2 spin echo intensities were first co-registered to their corresponding anatomic images. Second, co-registered T1w and T2w images were normalized to the MNI atlas using the deformation from 5f above and smoothed. The global signal levels were computed for each subject as the mean voxel value in a mask (brain region) generated using the voxel-based iterative sensitivity (VBIS) method.[25]

Image Comparison

Each image was first normalized either by the total GM volume, WM volume, global T1w level, or global T2w level. To perform VBM comparisons of *longitudinal difference* between CFS patients and NCs, temporal difference images were divided by the corresponding time between the two scan dates to generate rate-of-change images. Rate-of-change images from CFS patients were compared with those from NCs with a two sample t-test. The

significance of rate-of-change difference was tested using FWE corrected cluster level $P < 0.05$.

To perform *cross-sectional comparisons* between groups of CFS images and NC images *pooled* over the two time points, regional brain differences were determined with a two sample t-test. The significance of inter group difference was tested using FWE corrected cluster level $P < 0.05$. In addition to group comparisons, SPM regressions were performed against clinical measures of Bell CFS disability score, Somatic SS, and Neuro SS). All analyses incorporated the covariates of age, the appropriate global value (total GM volume, WM volume, global T1w level, or global T2w level), and HADS depression and anxiety scores. The significance of correlation was tested using family wise error (FWE) corrected cluster level $P < 0.05$.

Results

Optimization of Segmentation and VBM Options

The SPM12 segmentation with MRF of 4 rendered GM images that were closest to the manual segmentation results, i.e., highest median and smallest interquartile range for the Dice coefficient (Supp. Fig. S4). Table 1 summarizes the performance of the six VBM options. For sample sizes less than or equal to 15, the longitudinal approaches (LD and LJD) have higher sensitivity in preventing FN than DARTEL DN, DARTEL ST, and DARTEL SnPM. However, the LJD option also generates many FP inferences. The LD option was, therefore, optimal and was used here in VBM analysis of CFS and NC images.

Comparison of Clinical Measures and Global Volumes

For patients with CFS, mean longitudinal changes and correlations between time 1 and time 2 values for clinical measures and global GM and WM volumes are summarized in Table 2 (see Supp. Table S1 for those in NCs). There are significant decreases in total GM volume and increases in total WM volumes in both the CFS and NC groups (Table 2 and Supp. Table S1), although these longitudinal changes in total GM and WM volumes did not differ significantly between CFS and NC groups.

Table 3 summarizes means of clinical measures and total GM and WM volumes for pooled CFS and NC groups. There is no significant difference in total GM and WM volumes and ages between CFS and NC groups. All symptom scores are significantly different between CFS and NC groups. Bivariate correlations between any pair of clinical measures or total GM and WM volumes are summarized in Table 4. Pairs that are significantly correlated to each other are: total GM & WM volumes, depression and anxiety, and Neuro SS and somatic SS. In addition, total WM volumes were correlated with Somatic SS with uncorrected $P < 0.05$.

Different Longitudinal MRI Changes Between CFS and NC

The rate-of-change of regional WM volumes in CFS patients was significantly different from that in NCs in the

TABLE 1. Performance of VBM Methodological Options in Detection of Simulated Atrophy[a]

Methodological options	5% Atrophy				3% Atrophy				1% Atrophy			
	N = 25	N = 20	N = 15	N = 10	N = 25	N = 20	N = 15	N = 10	N = 25	N = 20	N = 15	N = 10
1. DARTEL DN	TP,FP	FN	FN	FN	FN	FN	FN	FN	FN	FN	FN	FN
2. DARTEL ST	TP	TP	FN	FN	TP	STP	FN, FP	FN, FP	TP	FN, FP	FN, FP	FN
3. SHOOT ST	TP	STP	FN	FN	STP	FN	FN	FN	STP	STP	FN	FN
4. DARTEL SnPM	TP, FP	TP, FP	FN, FP	FN	FN, FP	FN, FP	FN, FP	FN	FN, FP	FN, FP	FN, FP	FN
5. LD	TP	TP, FP	TP, FP	STP	TP	TP, FP	STP	FN	TP	TP	TP	FN
6. LJD	TP, FP	TP, FP	TP, FP	TP	TP, FP	TP, FP	TP	TP	TP, FP	TP, FP	TP, FP	TP, FP

[a]If not specified otherwise, default parameters/procedures were used. Default parameters/procedures include unified segmentation, creation of study specific templates, normalization to Montreal Neurological Institute (MNI) space, encoding of deformations as volume changes, smoothing with Gaussian kernel of 8mm × 8mm ×8mm, and parametric comparison. For an example, methodological option of DARTEL ST uses DARTEL registration to create a study specific template, normalizes final template MNI space, warps segmented images into MNI space, modulates volumetrics into intensities, smooths, and compares parametrically. Supplementary Figures S1 and S2 illustrated details of each option.
N = sample size; DARTEL = diffeomorphic anatomical registration through exponentiated lie algebra; DN = direct normalization; ST = study-specific template; SHOOT = geodesic shooting registration SnPM = statistical non-parametric mapping; LD = longitudinal difference; LJD = longitudinal Jacobian difference; TP = true positive; STP = small true positive; FN = false negative; FP = false positive.

TABLE 2. Mean Changes and Correlations between Values at Time 1 and Time 2 for Clinical Measures, Global GM Volumes, and Global WM Volumes in CFS[a]

Characteristics	Changes		Correlations	
	Mean (95% CI)	*P*	*r*	*P*
GM	18.6 ml (9.6, 27.6)	< 0.0071	0.98	< 0.0071
WM	−10 ml (−16.3, −3.7)	< 0.0071	0.98	< 0.0071
Bell score	−3 (−15, 10)	0.63	0.08	0.78
Depression	1 (−1, 4)	0.31	0.34	0.26
Anxiety	−2 (−4, 0)	0.07	0.51	0.07
Neuro SS	−4.8 (−8.7, −1)	0.02	0.4	0.14
Somatic SS	−6.6 (−11.2, −1.9)	0.009	0.45	0.09

[a]Changes were calculated as values at time 1 minus values at time 2 for each patient of chronic fatigue syndrome (CFS). GM and WM represent global gray matter (GM) and white matter (WM) volumes. Neuro SS and Somatic SS are neurological symptom score and somatic symptom score, respectively.
CI = confidence level; *P* = significance level; *r* = Pearson correlation coefficient.

left posterior part of the inferior fronto-occipital fasciculus (IFOF) and/or arcuate fasciculus (Fig. 2). In this location, WM volume relative to global WM volume decreased with time in the CFS group while in NCs it was unchanged.

Cross-sectional Differences in Pooled MR Images

The regional differences of GM and WM volumes and T1w and T2w signal intensities between *pooled* CFS and NC groups are summarized in Figure 3. In CFS, GM volumes were significantly decreased in the right inferior temporal gyrus and increased in the right supplementary motor area. The CFS group showed a significant decrease in WM volume in the left posterior part of IFOF/arcuate fasciculus. In the CFS group T1w signal intensities were significantly higher on the right in the parahippocampal gyrus, inferior temporal gyrus, and IFOF/arcuate fasciculus. T2w signal intensities were significantly higher in the right IFOF/arcuate fasciculus and inferior frontal gyrus regions in the CFS group.

Correlations of Pooled MR Images With Symptom Scores in CFS

Regional regression SPM results are summarized in Figure 4. Regional GM volume was significantly correlated with Neuro SS in the right fusiform gyrus positively and left superior parietal lobule negatively. Regional GM volume in the culmen was significantly and positively correlated with Somatic SS. Regional WM volume was significantly and positively correlated with Somatic SS in WM regions inferior to the left precentral sulcus. T2 signal intensities in left and right anterior IFOF/arcuate fasciculus were significantly and negatively correlated with Neuro SS.

Discussion

This study was designed to investigate longitudinal brain changes in CFS patients. The strength of the study is that we first validated SPM segmentation against manual segmentation and optimized VBM methodology for longitudinal analysis.

TABLE 3. Means of Clinical Measures and Global GM and WM Volumes of Pooled CFS and NC Groups

Characteristics	$M_{CSF} \pm SD$	$M_{NC} \pm SD$	*P*
GM	659 ± 72.6 ml	693.5 ± 83.5 ml	0.14
WM	492.7 ± 58.9 ml	502.3 ± 43.3 ml	0.51
Age	37.28 ± 9.63 yrs.	33.8 ± 8.67 yrs.	0.19
Bell score	46.2 ± 15.3	99 ± 3.1	< 0.0062
Depression	7 ± 4	3 ± 3	< 0.0062
Anxiety	7 ± 3	3 ± 3	< 0.0062
Neuro SS	20.35 ± 6.72	35.5 ± 3.41	< 0.0062
Somatic SS	32.88 ± 8.51	55.52 ± 3.06	< 0.0062

GM = gray matter; WM = white matter; CFS = chronic fatigue syndrome; NC = normal control; M = mean value; *P* = significance level; Neuro SS = neurological symptom score; Somatic SS = somatic symptom score.

TABLE 4. Bivariate Correlations among Clinical Measures and the Total GM and WM Volumes

Characteristics	GM	WM	Bell score	Depression	Anxiety	Neuro SS	Somatic SS
GM							
WM	0.68[a]						
Bell score	0.14	0.24					
Depression	0.02	0.31	-0.29				
Anxiety	0.02	0.26	0.07	0.56[a]			
Neuro SS	0.04	0.19	0.56[a]	-0.31	0.05		
Somatic SS	0.13	0.41[b]	0.69[a]	-0.15	0.26	0.54[a]	

GM = gray matter; WM = white matter; Neuro SS = neurological symptom score; Somatic SS = somatic symptom score.
[a]$P < 0.002$.
[b]$P < 0.05$.

We found for the first time that, over a period of 6 years, regional WM volume decreases in the left IFOF/arcuate fasciculus in CFS patients while remaining stable in NCs. This longitudinal WM finding was consolidated by cross-sectional analysis of the pooled CFS and NC groups. Inter-group comparison found decreased GM and WM volumes and increased T1w and increased T2w intensities (which may reflect decreased blood volumes and ischemia) near this ILOF/arcuate

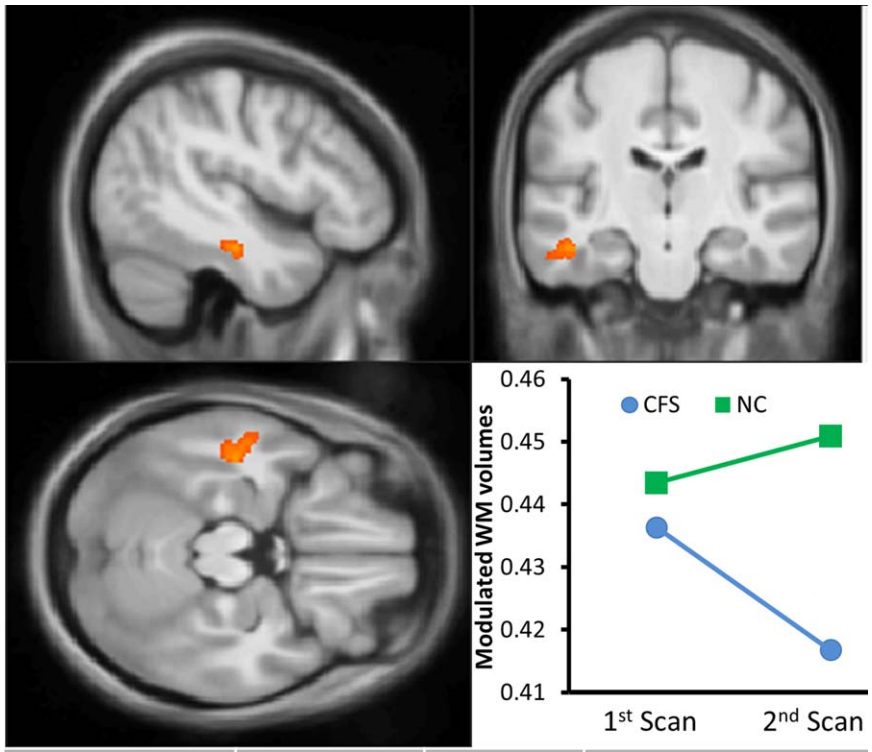

FIGURE 2: Voxel-based morphometry (VBM) of white matter (WM) longitudinal change rate difference between chronic fatigue syndrome (CFS) and normal control (NC) subjects. The significant cluster is superimposed on sections through its peak voxel of the average 3D T1 weighted image from this study. The plot shows the mean modulated WM volume at time points 1 and 2 in the CFS and NC groups. $P_{FWE\_corr\_cluster}$ is the family wise error (FWE) corrected cluster *P* value; *k* is the size of cluster in voxels; *T* statistic value is the rate difference relative to the temporal change rate variance.

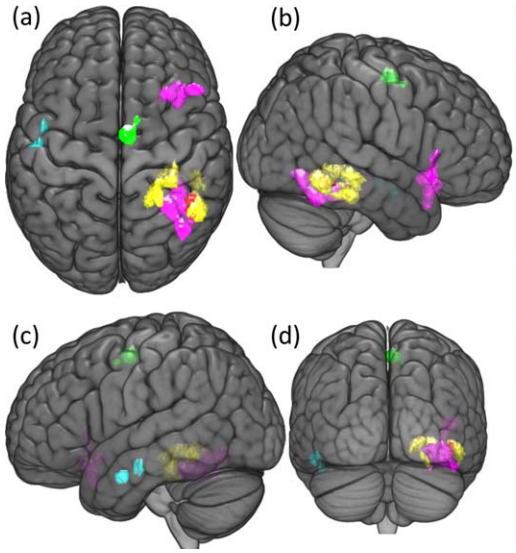

Features	P_{FWE}	k	T	MNI
GM vol: CFS > NC (green)	0.02	271	5.84	4 -6 52
GM vol: CFS < NC (red)	0.02	197	6.2	48 -48 -10
WM vol: CFS < NC (cyan)	0.02	80	6.1	-52 -12 -18
T1: CFS > NC (yellow)	0.008	786	4.77	28 -32 -16
T1: CFS > NC (yellow)	0.03	606	5.62	48 -56 -8
T2: CFS > NC (magenta)	< 0.001	1246	5.05	40 -64 -9
T2: CFS > NC (magenta)	0.02	526	5.34	45 22 6

FIGURE 3: Regional differences of gray matter (GM) and white matter (WM) volumes and T1w and T2w signal intensities between CFS and NC groups. Maximum intensity projections of T statistic clusters that are significantly different between CFS group and NCs were superimposed on a 3D rendering of T1 weighted images in Montreal Neurological Institute (MNI) space. The 3D rendered image was set to transparent to reveal underlaying clusters: top view (a), right view (b), left view (c), and posterior view (d). Characteristics of significant clusters are summarized in the side table, in which P_{FWE} is the family wise error (FWE) corrected cluster *P* value; *k* is the size of the cluster in voxels; *T* is the difference relative to the variation; and MNI refers to the MNI coordinates.

area both ipsi- and contra-laterally. Furthermore, regional GM and T2w (blood volumes) were positively correlated with the Neuro and Somatic Symptom Scores in the same areas and elsewhere.

VBM is a commonly used automated tool for studying patterns of brain change in neurological diseases and neuroanatomical correlates of subject characteristics. Although most VBM processing and analysis is automated in SPM, several methodological options remain for user specification,[19] especially in analysis of longitudinal image data. Inconsistent VBM findings in CFS patients in previous studies[6,7,12,14] motivated us here to validate segmentation and optimize VBM methodology. The VBM atrophy simulation experiment demonstrated (1) that normalization to a

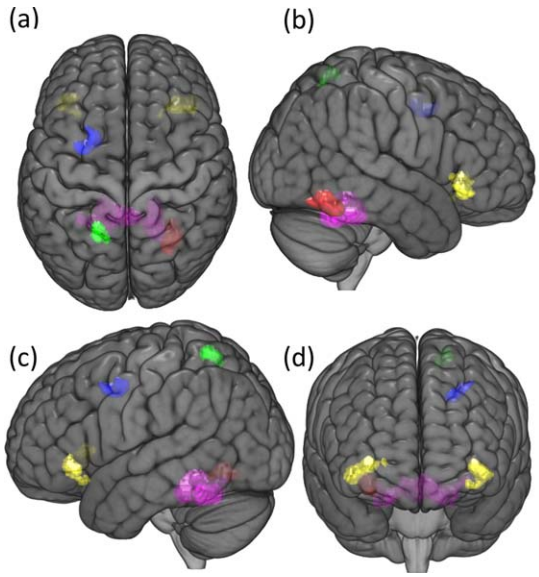

Regressions	P_{FWE}	k	T	MNI
GM vol vs NeuroSS (+) (red)	0.006	599	6.76	27 -60 -15
GM vol vs NeuroSS (-) (green)	0.006	286	6.8	-18 -56 64
GM vol vs SomaticSS (+) (magenta)	< 0.001	3115	6.51	-2 -48 -22
WM vol vs SomaticSS (+) (blue)	0.03	371	4.94	-21 6 40
T2 vs NeuroSS (-) (yellow)	0.01	393	5.61	-38 32 -6
T2 vs NeuroSS (-) (yellow)	0.02	562	5.61	32 27 0

FIGURE 4: Clusters from regressions of regional gray matter (GM) and white matter (WM) volumes and T1w and T2w signal intensities versus clinical measures in the pooled CFS group. Maximum intensity projections of T statistic clusters that are significantly correlated with clinical measures were superimposed on a 3D rendering of T1 weighted images in Montreal Neurological Institute (MNI) space. The 3D rendered image was set to transparent to reveal underlaying clusters: top view (a), right view (b), left view (c), and posterior view (d). Characteristics of significant clusters are summarized in the side table, in which P_{FWE} is the family wise error (FWE) corrected cluster *P* value; *k* is the size of cluster in voxels; *T* is the correlation coefficient relative to the standard error; and MNI refers to the MNI coordinates; "+" and "-" represent positive and negative correlations, respectively.

study specific template performs better than direct normalization to the default template provided in SPM12; (2) when the sample size is small, a random effects one-sample t-test of longitudinal difference images, either by means of the Jacobian difference method or the direct difference between different time points, has higher sensitivity than a paired t-test of images from two time points; (3) that creation of a single image representative of the two time points (within-subject template) for the purpose of the shared final spatial normalization should involve similar normalizations of both raw images and the same processing steps.

This study detected continuing shrinkage of WM in the left IFOF in patients with CFS, but not in NCs. This result was consolidated by the pooled inter group comparisons revealing decreased regional WM volumes in adjacent regions and decreased GM and blood volumes in contralateral regions and by regression analysis showing significant correlations of WM and GM volumes and T2w intensities with CFS symptom scores in those regions. The superficial and dorsal subcomponent of the IFOF connects the frontal lobe with the superior parietal lobe and the ventral subcomponent of the IFOF connects the frontal lobe with the inferior occipital lobe and temporo-basal area.[26] Therefore, our findings are consistent with the decreased intrinsic connectivity in CFS within left fronto-parietal networks (FPN) found in a resting-state functional connectivity study.[27] Similarly, a diffusion tensor imaging (DTI) study reported bilateral white matter atrophy and increased fractional anisotropy in the arcuate fasciculus, possibly reflecting degeneration of cross fibers.[8]

The IFOF connects networks of cognitive control, attention, language processing, and working memory[28] and links the bilateral insular regions and anterior cingulate cortex.[29] Considerable evidence suggested that the IFOF plays a pivotal role as the connectivity substrate in goal-directed cognition, mediating the dynamic balance between default mode network and dorsal attention networks.[30] Therefore, symptoms experienced by CFS patients, such as impaired concentration, working memory loss, inability to focus vision, and poor motor coordination could be explained, in part at least, by our finding of continuing shrinkage of WM in the IFOF. Our finding of IFOF WM shrinkage in CFS, together with consistent findings by us and others above, warrants more investigations to understand the pathomechanism of this deficit.

Compared with NC, CFS patients also showed decreased GM volume and increased T1w and T2w signal intensities near the contralateral ILOF. The absence of corresponding longitudinal findings in the right hemisphere may be a result of lower sensitivity in longitudinal studies and/or because the changes in CFS occurred soon after onset (before the first scan) and did not progress appreciably thereafter. The increased T2w signal intensities suggest possible decreased blood volume in these regions.[31] Indeed, previous studies have found decreased regional cerebral blood flow in frontal and temporal lobes[32] and decreased frontal oxygenation[33] in patients with CFS. Thus, a gradual and chronic hypoperfusion of the brain may contribute to this continuing WM shrinkage.

Additionally, chronic functional hypoxia due to dysfunction of the neurovascular unit could also cause neurodegeneration.[34] Of interest, a recent study found seventeen single nucleotide polymorphisms (SNPs) were significantly associated with CFS.[35] Nine of these SNPs were associated with muscarinic acetylcholine receptors and eight with nicotinic ACh receptors (nAChRs). ACh, a neuromodulator in the brain, changes the state of neuronal networks throughout the brain and modifies their response to internal and external inputs. Control of synaptic Ca^{2+} concentration following nAChR stimulation is a major pathway for ACh to influence neuronal networks.[36] Furthermore, nAChRs are also present in the cerebral vascular endothelium and smooth muscles.[37] Thus, aberrant AChR function may impair cerebrovascular autoregulation and cause chronic functional hypoxia. Distribution of moderate nAChR density in temporal parietal cortices and low levels in white matter tracts could make IFOF more vulnerable to aberrant AChR function. Furthermore, the IFOF is in a brain region that undergoes continued organization in early adulthood[38] and is particularly vulnerable to vascular risk factors.[39]

Regression analysis also showed several image measures correlated with symptom scores in regions other than the IFOF. These findings are consistent with existing knowledge of brain structure-function relationships. For example, regional GM volumes are positively correlated with Neuro SS in the right fusiform gyrus, which is involved with brain recognition functions. Similarly, low regional GM volumes in the culmen of cerebellum and low regional WM volumes inferior to precentral sulcus are correlated with impaired somatic status.

The inter-group comparison and regression analysis showed that CFS patients had increased regional GM volume in the supplementary motor area and this regional GM volume is negatively correlated with Neuro SS, i.e., higher regional GM volume with more severe symptoms. These findings are in line with the clinical observation that CFS patients need extra effort for motor coordination, with fMRI results that CFS patients recruit more cerebral regions for tasks,[40] and with increased cortical thickness in CFS in the precentral gyrus.[8] We postulate that these increased regional GM volumes may be a result of brain plasticity compensating for communication deficits because of WM shrinkage.

This study has several limitations. We found continuing shrinkage of WM volume in posterior IFOF region in CFS patients. Although several tracts could be affected in

this area, we postulated that the IFOF was mainly involved based on previous fMRI studies.[27] Therefore, it is still necessary to identify and confirm deficits in WM fiber tracts using DTI. Indeed, we are currently acquiring DTI and fMRI data to identify affected WM tracts and to investigate functional consequences of these deficits. Two symptom severity scores, Somatic and Neuro SS, used in this study are based on the most frequent CFS symptoms[16] and, although not validated, have much in common with validated scores, such as the Center for Disease Control CFS symptom inventory. The study was designed to investigate progressive brain changes with an interval between the two scans of 6 years. The first scan included 25 CFS patients and 25 NCs, but because of the relatively long interval, only 15 CFS patients and 10 NCs returned for the second scan. Although we detected progressive WM atrophy in the IFOF region in CFS patients, because of our small sample size and low detection power, we cannot rule out progressive changes elsewhere that are specific to CFS.

In conclusion, we optimized VBM for longitudinal analysis and for the first time found continuing WM shrinkage in the left posterior IFOF in CFS patients but not NCs, using MR data acquired with a 6-year gap. The longitudinal finding was consolidated by the decreased regional GM, WM, and blood volumes in adjacent regions. Furthermore, these regional GM and WM volumes were significantly correlated with symptom scores. The results suggest that CFS is a chronic illness with abnormal connections among brain regions and WM deficits which continue to deteriorate post onset. This study warrants further investigations to understand the pathomechanism of WM deficits in the IFOF in CFS.

Acknowledgment

Contract grant sponsor: Judith Jane Mason Foundation
The funding sources had no involvement in the design of this study.

References

1. Working Group of the Royal Australasian College of Physicians. Chronic fatigue syndrome. Clinical practice guidelines--2002. Med J Aust 2002;176(Suppl):S23–S56.
2. Carruthers BM, Jain AK, De Meirleir KL, et al. Myalgic encephalomyelitis/chronic fatigue syndrome: clinical working case definition, diagnostic and treatment protocols. J Chronic Fatigue Syndr 2003;11:7–115.
3. Fukuda K, Straus SE, Hickie I, Sharpe MC, Dobbins JG, Komaroff A. The chronic fatigue syndrome: a comprehensive approach to its definition and study. Ann Intern Med 1994;121:953–959.
4. Holgate S, Komaroff A, Mangan D, Wessely S. Chronic fatigue syndrome: understanding a complex illness. Nat Rev Neurosci 2011;12:539–544.
5. Barnden L, Kwiatek R, Crouch B, et al. Autonomic correlations with MRI are abnormal in the brainstem vasomotor centre in Chronic Fatigue Syndrome. NeuroImage: Clinical 2016;11:530–537.
6. de Lange F, Kalkman J, Bleijenberg G, Hagoort P, van der Meer J, Toni I. Gray matter volume reduction in the chronic fatigue syndrome. Neuroimage 2005;26:777–781.
7. Okada T, Tanaka M, Kuratsune H, Watanabe Y, Sadato N. Mechanisms underlying fatigue: a voxel-based morphometric study of chronic fatigue syndrome. BMC Neurol 2004;4:14–19.
8. Zeineh MM, Kang J, Atlas SW, et al. Right arcuate fasciculus abnormality in chronic fatigue syndrome. Radiology 2015;274:517–526.
9. Perrin R, Embleton K, Pentreath V, Jackson A. Longitudinal MRI shows no cerebral abnormality in chronic fatigue syndrome. Br J Radiol 2010;83:419–423.
10. de Lange F, Koers A, Kalkman J, et al. Increase in prefrontal cortical volume following cognitive behavioural therapy in patients with chronic fatigue syndrome. Brain 2008;131:2172–2180.
11. Barnden L, Crouch B, Kwiatek R, et al. A brain MRI study of chronic fatigue syndrome: evidence of brainstem dysfunction and altered homeostasis. NMR Biomed 2011;24:1302–1312.
12. Puri BK, Jakeman PM, Agour M, et al. Regional grey and white matter volumetric changes in myalgic encephalomyelitis (chronic fatigue syndrome): a voxel-based morphometry 3 T MRI study. Br J Radiol 2012;85:e270–e273.
13. Lange G, Holodny A, DeLuca J, et al. Quantitative assessment of cerebral ventricular volumes in chronic fatigue syndrome. Appl Neuropsychol 2001;8:23–30.
14. Barnden L, Crouch B, Kwiatek R, Burnet R, Del Fante P. Evidence in chronic fatigue syndrome for severity-dependent upregulation of prefrontal myelination that is independent of anxiety and depression. NMR Biomed 2015;28:404–413.
15. Bell DS. The doctor's guide to chronic fatigue syndrome. Reading, MA: Addison Wesley; 1995.
16. Hawk C, Jason L, Torres-Harding S. Reliability of a chronic fatigue syndrome questionnaire. J Chronic Fatigue Syndr 2006;13:41–66.
17. Zigmond A, Snaith R. The Hospital Anxiety and Depression scale. Acta Psychiatr Scand 1983;67:361–370.
18. Ashburner J, Friston KJ. Unified segmentation. Neuroimage 2005;26:839–851.
19. Ridgway GR, Henley SM, Rohrer JD, Scahill RI, Warren JD, Fox NC. Ten simple rules for reporting voxel-based morphometry studies. NeuroImage 2008;40:1429–1435.
20. Karacali B, Davatzikos C. Simulation of tissue atrophy using a topology preserving transformation model. IEEE Trans Med Imaging 2006;25:649–652.
21. Ashburner J. A fast diffeomorphic image registration algorithm. Neuroimage 2007;38:95–113.
22. Ashburner J, Friston KJ. Diffeomorphic registration using geodesic shooting and Gauss-Newton optimisation. Neuroimage 2011;55:954–967.
23. Holmes AP, Blair RC, Watson JD, Ford I. Nonparametric analysis of statistic images from functional mapping experiments. J Cereb Blood Flow Metab 1996;16:7–22.
24. Ashburner J, Ridgway GR. Symmetric diffeomorphic modeling of longitudinal structural MRI. Front Neurosci 2012;6:197.
25. Abbott D, Pell G, Pardoe H, Jackson G. Voxel-Based Iterative Sensitivity (VBIS): methods and a validation of intensity scaling for T2-weighted imaging of hippocampal sclerosis. Neuroimage 2009;44:812–819.
26. Martino J, Brogna C, Robles SG, Vergani F, Duffau H. Anatomic dissection of the inferior fronto-occipital fasciculus revisited in the lights of brain stimulation data. Cortex 2010;46:691–699.
27. Gay CW, Robinson ME, Lai S, et al. Abnormal resting-state functional connectivity in patients with chronic fatigue syndrome: results of seed and data-driven analyses. Brain connectivity 2016;6:48–56.

28. Lois G, Linke J, Wessa M. Altered functional connectivity between emotional and cognitive resting state networks in euthymic bipolar I disorder patients. PLoS One 2014;9:e107829.

29. Dosenbach NU, Fair DA, Miezin FM, et al. Distinct brain networks for adaptive and stable task control in humans. Proc Natl Acad Sci U S A 2007;104:11073–11078.

30. Vallesi A, Arbula S, Capizzi M, Causin F, D'Avella D. Domain-independent neural underpinning of task-switching: an fMRI investigation. Cortex 2015;65:173–183.

31. Ginat DT, Meyers SP. Intracranial lesions with high signal intensity on T1-weighted MR images: differential diagnosis. Radiographics 2012; 32:499–516.

32. Schwartz R, Komaroff A, Garada B, et al. Comparison of findings in patients with chronic fatigue syndrome, AIDS dementia complex, and major unipolar depression. AJR Am J Roentenol 1994;162:943–951.

33. Patrick Neary J, Roberts AD, Leavins N, Harrison MF, Croll JC, Sexsmith JR. Prefrontal cortex oxygenation during incremental exercise in chronic fatigue syndrome. Clin Physiol Funct Imaging 2008;28: 364–372.

34. Zacchigna S, Lambrechts D, Carmeliet P. Neurovascular signalling defects in neurodegeneration. Nat Rev Neurosci 2008;9:169–181.

35. Marshall-Gradisnik S, Smith P, Nilius B, Staines DR. Examination of single nucleotide polymorphisms in acetylcholine receptors in chronic fatigue syndrome patients. Immunol Immunogenet Insights 2015;7:7.

36. Takata N, Mishima T, Hisatsune C, et al. Astrocyte calcium signaling transforms cholinergic modulation to cortical plasticity in vivo. J Neurosci 2011;31:18155–18165.

37. Bruggmann D, Lips KS, Pfeil U, Haberberger RV, Kummer W. Rat arteries contain multiple nicotinic acetylcholine receptor alpha-subunits. Life sciences 2003;72:2095–2099.

38. Bava S, Thayer R, Jacobus J, Ward M, Jernigan TL, Tapert SF. Longitudinal characterization of white matter maturation during adolescence. Brain Res 2010;1327:38–46.

39. Maillard P, Seshadri S, Beiser A, et al. Effects of systolic blood pressure on white-matter integrity in young adults in the Framingham Heart Study: a cross-sectional study. Lancet Neurol 2012;11:1039–1047.

40. de Lange F, Kalkman J, Bleijenberg G, et al. Neural correlates of the chronic fatigue syndrome - an fMRI study. Brain 2004;127:1948–1957.